RAST: Reasoning Activation in LLMs via Small-model Transfer

Siru Ouyang[1], Xinyu Zhu[2], Zilin Xiao[3], Minhao Jiang[4], Yu Meng[2], Jiawei Han[1]
[1] University of Illinois Urbana-Champaign, [2] University of Virginia
[3] Rice University, [4] GE HealthCare
siruo2@illinois.edu

Abstract

Reinforcement learning (RL) has become a powerful approach for improving the reasoning capabilities of large language models (LLMs), as evidenced by recent successes such as OpenAI's o1 and Deepseek-R1. However, applying RL at scale remains intimidatingly resource-intensive, requiring multiple model copies and extensive GPU workloads. On the other hand, while being powerful, recent studies suggest that RL does not fundamentally endow models with new knowledge; rather, it primarily reshapes the model's output distribution to activate reasoning capabilities latent in the base model. Building on this insight, we hypothesize that the changes in output probabilities induced by RL are largely model-size invariant, opening the door to a more efficient paradigm: training a small model with RL and transferring its induced probability shifts to larger base models. To verify our hypothesis, we conduct a token-level analysis of decoding trajectories and find high alignment in RL-induced output distributions across model scales, validating our hypothesis. Motivated by this, we propose RAST, a simple yet effective method that transfers reasoning behaviors by injecting RL-induced probability adjustments from a small RL-trained model into larger models. Experiments across multiple mathematical reasoning benchmarks show that RAST substantially and consistently enhances the reasoning capabilities of base models while requiring significantly lower GPU memory than direct RL training, sometimes even yielding better performance than the RL-trained counterparts. Our findings offer new insights into the nature of RL-driven reasoning and practical strategies for scaling its benefits without incurring its full computational cost. The project page of RAST is available at https://ozyyshr.github.io/RAST/.

1 Introduction

Reinforcement learning (RL) [25, 59] has emerged as a powerful and prevalent paradigm for enhancing the reasoning capabilities of large language models (LLMs) [16, 49, 66, 53]. Notably, recent successes such as OpenAI's o1 model [23] and Deepseek-R1 [14] have demonstrated substantial improvements through learning from oracle-verified feedback, employing advanced RL algorithms including Proximal Policy Optimization (PPO) [52] and Group Relative Policy Optimization (GRPO) [54]. However, RL is notoriously inefficient and resource-intensive [55] — it requires loading multiple copies of the same-sized models (e.g., policy, critic, reference, reward) with extensive training GPU memory workloads. Additionally, traditional RL algorithms (e.g., PPO) typically require multiple iterations, each involving interdependent stages such as rollout, replay, and optimization [31].

On the other hand, recently, there have been a bunch of works studying behaviors of RL-trained models, aiming to answer the question, *"how does RL elicit reasoning capabilities in LLMs?"* [43, 54,

Preprint. Under review.

Model Scale	PCR
7B	96.03
14B	95.60
32B	95.22

(a) PCR for different model scales

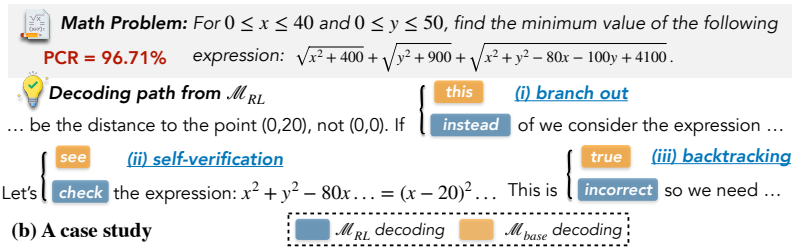

(b) A case study

Figure 1: *(a) PCR (path coverage rate) across different model scales. (b) A case study* revealing the decoding path of $\mathcal{M}_{\text{base}}$ and its RL-trained version $\mathcal{M}_{\text{RL}}$. Only a very small subset of tokens differ on the decoding path between $\mathcal{M}_{\text{base}}$ and $\mathcal{M}_{\text{RL}}$, which indicates particular reasoning behaviors.

4]. It is increasingly believed that RL does not endow LLMs with fundamentally new knowledge [70, 12]. Instead, it serves to elicit and amplify reasoning behaviors already present within base models [74, 40, 8]. For example, branching out for alternative solution paths, backtracking from incorrect steps [11, 50], and self-verification for generation [60]. The aforementioned studies lead to a major hypothesis [33] in our paper as follows:

> **Hypothesis:** RL activates latent reasoning capabilities in LLMs not by globally altering the entire output distribution, but by selectively adjusting the probabilities of a small subset of tokens that correspond to key reasoning behaviors. The majority of token probabilities — which encode core knowledge and reasoning content — remain largely unchanged.

Specifically, if RL primarily teaches models reasoning behaviors (*how* to reason) by modulating output probabilities rather than imparting fundamentally new knowledge or concepts (*what* to reason), then the adjustments learned through RL should inherently reflect reasoning skills already latent within base models. This reasoning-centric view suggests that these learned adjustments may not strongly depend on specific model scales or capacities. Consequently, this hypothesis presents a significant opportunity: applying RL to smaller, computationally efficient models and subsequently transferring the learned probabilistic adjustments to larger, more capable models. Such an approach could substantially mitigate the prohibitive computational and financial costs associated with directly performing RL on large-scale models.

We test our hypothesis via a preliminary study that compares the token-level decoding path shifts between base $\mathcal{M}_{\text{base}}$ and RL-trained models $\mathcal{M}_{\text{RL}}$ [1] of varying sizes. As illustrated in Figure 1(b), $\mathcal{M}_{\text{RL}}$ introduces only minimal shifts in the decoding path, with around 96.71% of tokens remaining unchanged in this specific case. Notably, these shifts are highly localized to a few reasoning-critical tokens, such as those triggering self-verification, branching out, or backtracking. This suggests that RL acts by amplifying latent reasoning behaviors rather than rewriting entire outputs.

Inspired by the above findings, we propose a simple and intuitive method, RAST, which leverages shifts in the output space to transfer learned "reasoning patterns" from a small RL-trained model (relative to its base) to larger base models across different scales. Extensive experimental results show that RAST substantially and consistently enhances the reasoning capabilities of base models, while requiring significantly lower GPU memory than direct RL training. Surprisingly, sometimes RAST yield even better performance than the RL-trained counterparts. Additionally, RAST also increases search space diversity compared to conventional RL training, exemplified by the superior pass@k performance. We further conduct detailed analyses on why RAST works and provide insights and practical guidelines for applying RAST, hoping to shed light on future works in this research line.

2 Methodology

Our goal is to enable a large base model $\mathcal{M}_{\text{base}}$ to emulate the reasoning behavior of a smaller reasoner $\mathcal{S}_{\text{RL}}$ tuned with RL, without requiring expensive RL training at scale. To this end, we begin with a preliminary study that motivates our core hypothesis and then introduce *reasoning activation via small-model transfer*, termed as RAST, a simple yet effective decoding-time method that activates reasoning capabilities across model scales.

[1] Unless otherwise specified, all mentions of RL-trained models in this paper refer to "RL from scratch" [72], directly training models using RL from the base model without SFT warmup.

2.1 Preliminary Study

We begin with a preliminary study to empirically support our *hypothesis* from Sec. 1 — RL activates reasoning capabilities in LLMs by adjusting the probabilities of *a small set of key tokens* that relate to particular reasoning behaviors. Concretely, we take the decoding path $T = [t_1, t_2, ..., t_n]$ from $\mathcal{M}_{\text{RL}}$, and feed it into $\mathcal{M}_{\text{base}}$ token by token to see if the next token prediction t'_{i+1} aligns with t_{i+1} (i.e., $\mathcal{M}_{\text{base}}$ generates the t_{n+1}-th token based on the first n tokens generated by $\mathcal{M}_{\text{RL}}$, regardless of the previous $\mathcal{M}_{\text{base}}$ generated tokens):

$$t'_{i+1} = \arg\max_t P_{\mathcal{M}_{\text{base}}}(t \mid t_1, \ldots, t_i) \stackrel{?}{=} t_{i+1} \tag{1}$$

This setup enables us to quantify how likely $\mathcal{M}_{\text{base}}$ is to recover the RL path. This study is conducted under greedy decoding to avoid potential randomness. To capture this alignment quantitatively, we define *Path Coverage Rate (PCR)* as the proportion of tokens in T for which the base model exactly matches the RL output:

$$\text{PCR}(T) = \frac{1}{n-1} \sum_{i=1}^{n-1} \mathbb{I}\left[t'_{i+1} = t_{i+1}\right] \tag{2}$$

A high PCR indicates that the $\mathcal{M}_{\text{base}}$ is already well-aligned with the RL decoding path, with only minor adjustments needed to activate desired reasoning behaviors. In our implementation, Qwen-2.5-32B-SimpleRL-Zoo serves as $\mathcal{M}_{\text{RL}}$ and Qwen2.5-32B is used as $\mathcal{M}_{\text{base}}$. We randomly sampled 50 trajectories from $\mathcal{M}_{\text{RL}}$ from MATH500 [18] and took the sample-level average as the final results. As shown in Figure 1(a), we observe that PCR remains remarkably high ($> 95\%$) across all model scales, indicating that RL-induced distributional shifts are notable only on a small set of tokens, with the majority of tokens also predictable by $\mathcal{M}_{\text{base}}$. Additionally, we found that the disparities mainly come from tokens that reflect certain reasoning behaviors. This indicates that by steering around these key tokens, $\mathcal{M}_{\text{base}}$ is able to recover the reasoning path generated by the RL-trained model.

2.2 RAST: Reasoning Activation in LLMs via Small-model Transfer

Building on the findings from our preliminary study, we hypothesize that minor, targeted adjustments to the $\mathcal{M}_{\text{base}}$'s output distribution can effectively enable it to perform on par with its RL-trained counterpart, without the need for expensive RL optimization directly conducted upon the large base model. In other words, we aim to transform $\mathcal{M}_{\text{base}}$ into a stronger reasoner at inference time by activating the latent reasoning capabilities already present within it in the token/output space.

To this end, we propose RAST, a decoding-time method that activates reasoning capabilities in large models by transferring logit-level adjustments from smaller RL-tuned models. Given the smaller model pair $\mathcal{S}_{\text{base}}$ and $\mathcal{S}_{\text{RL}}$, we propose leveraging their differences in logit distributions as reusable reasoning correction signals. Specifically, at the decoding time stamp t, with previous input as $x_{<t}$, we compute the logit scores of $\mathcal{M}_{\text{base}}$, $\mathcal{S}_{\text{base}}$, $\mathcal{S}_{\text{RL}}$, and define the final probability distribution over tokens for the enhanced model $\tilde{\mathcal{M}}$ as:

$$P_{\tilde{\mathcal{M}}}(X_t \mid x_{<t}) = \text{softmax}\left[\mathcal{M}_{\text{base}}(X_t \mid x_{<t}) + \lambda(\mathcal{S}_{\text{RL}}(X_t \mid x_{<t}) - \mathcal{S}_{\text{base}}(X_t \mid x_{<t}))\right] \tag{3}$$

where the adjustment terms represent the difference in token-level scoring between the RL-trained model and its base counterpart, denoted as ΔR. λ controls the strengths of ΔR. These logits encode reasoning-oriented shifts that can be transferred to the larger base model, allowing it to mimic improved inference behavior without retraining. Figure 2 outlines the overview of RAST, showing how ΔR from a small RL-tuned model is injected to adjust the output distribution of $\mathcal{M}_{\text{base}}$ at decoding time, selectively amplifying reasoning-relevant tokens (e.g., "instead") while preserving base predictions (e.g., "of") elsewhere. The additive formulation enables lightweight adaptation at inference time by altering the output distribution in a way that reflects reasoning preferences learned by the smaller model.

Our method is conceptually related to [35, 36, 30], which apply similar manipulation in logits spaces for generation steering. However, while these methods are often task-specific or used for controlling style/toxicity, our focus is on eliciting complex reasoning behavior, and we demonstrate that even small-scale reasoning signals can be reliably transferred across model sizes and domains.

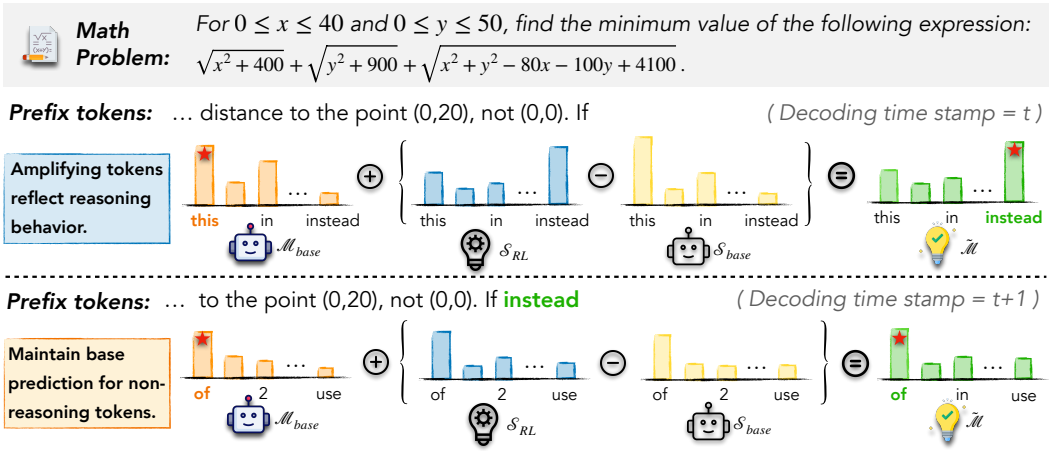

Figure 2: A concrete illustration of RAST: logit differences from a small RL-tuned model $\mathcal{S}_{\text{RL}}$ guide a large base model $\mathcal{M}_{\text{base}}$ at decoding time, amplifying reasoning-relevant predictions (e.g., "instead") while maintaining base outputs for non-reasoning tokens (e.g., "of").

3 Unlocking Reasoning Activation

3.1 Experimental Setup

Models and Tasks We systematically evaluate model performance across a comprehensive suite of mathematical reasoning tasks of varying difficulty, including standard benchmarks such as MATH500 [18], Minerva [29], OlympiadBench [17], GSM8K [6], as well as competition-level benchmarks AIME24 and AMC23. Our primary models are from the Qwen-2.5 family (1.5B, 7B, 14B, and 32B) [67] alongside their corresponding RL-trained variants using SimpleRL-Zoo [72] (e.g., SimpleRL-7B denotes the "RL from scratch" variant of Qwen-2.5-7B). We further demonstrate the generalizability of RAST across different model architectures and downstream tasks. To validate this, we conduct experiments using the Llama-3.1 series (8B, 70B) [13] and their zero RL-trained counterparts. Additionally, we assess model performance on coding tasks, utilizing zero RL-trained models from Code-R1 [39] trained from Qwen-2.5-1M [68] on coding benchmarks including HumanEval [2], MBPP+ [1], and LiveCodeBench [24]. For details of datasets and setup used in our experiments, please refer to Appendix A. We also present additional experiments and analysis results in Appendix C.

Evaluation Metrics Following previous work [19], and to ensure rigorous evaluation across models and tasks, we perform inference runs k up to 32 for each experimental setup and report the following metrics calculated over the collected trajectories:

- **Pass@k**: Pass@k evaluates whether at least one correct solution is found among k sampled outputs per problem. Formally,

$$\text{Pass@}k = \frac{1}{N}\sum_{i=1}^{N}\mathbb{I}\left(\sum_{j=1}^{k}\mathbb{I}\left(\hat{y}_{i,j}=y_i\right)\geq 1\right), \tag{4}$$

  where N is the total number of problems, $\hat{y}_{i,j}$ is the prediction for the i-th problem in the j-th run, y_i is the corresponding ground truth, and $\mathbb{I}(\cdot)$ denotes the indicator function.[2]

- **Recovery Rate**: The recovery rate quantifies how much of the gap between the base model and a stronger RL-tuned model is recovered by the proposed method. Formally,

$$\text{Recovery Rate} = \frac{\text{Accuracy}_{\text{RAST}} - \text{Accuracy}_{\text{Base}}}{\text{Accuracy}_{\text{RL}} - \text{Accuracy}_{\text{Base}}}, \tag{5}$$

  where "Accuracy" denotes the averaged pass@1 over 32 runs. Higher values of *recovery rate* indicate a more effective recovery of the performance gap.

[2]We use the same answer extraction and matching for performance evaluation as SimpleRL, following https://github.com/hkust-nlp/simpleRL-reason/tree/v1/examples/simplelr_math_eval.

Table 1: Experiment results of RAST on mathematical reasoning datasets with Qwen-2.5 model series. All numbers are computed across 32 runs with sampling, except that all base models use greedy decoding. *Avg.* indicates the averaged *pass@1* over 32 runs and *RR.* denotes the recovery rate.

Models	Math500		AIME24		AMC		Minerva		Olympiad		GSM8K	
	Avg.	*RR.*	*Avg.*	*RR.*	*Avg.*	*RR.*	*Avg.*	*RR.*	*Avg.*	*RR.*	*Avg.*	*RR.*
Qwen-2.5-32B	68.6	-	3.3	-	52.5	-	21.0	-	33.1	-	93.1	-
$+\Delta R_{1.5B}$ †	73.7	40.2%	12.5	37.9%	54.7	12.9%	25.1	84.1%	36.7	30.5%	93.3	7.7%
$+\Delta R_{7B}$	79.0	81.9%	16.4	53.9%	58.4	34.5%	32.0	87.3%	41.7	72.9%	94.4	50.0%
$+\Delta R_{14B}$	80.7	95.3%	18.3	61.7%	65.2	74.3%	34.2	104.8%	43.5	88.1%	95.3	84.6%
SimpleRL-32B	81.3	-	27.6	-	69.6	-	33.6	-	44.9	-	95.7	-
Qwen-2.5-14B	63.8	-	6.7	-	47.5	-	19.1	-	31.1	-	91.4	-
$+\Delta R_{1.5B}$ †	70.3	45.1%	10.9	54.5%	50.3	25.0%	22.9	29.0%	35.5	37.0%	92.4	31.3%
$+\Delta R_{7B}$	77.4	94.4%	16.2	123.4%	56.1	76.8%	28.8	74.0%	40.0	75.4%	93.3	59.4%
SimpleRL-14B	78.2	-	14.4	-	58.7	-	32.2	-	42.9	-	94.6	-
Qwen-2.5-7B	62.9	-	6.7	-	32.5	-	19.9	-	28.0	-	87.7	-
$+\Delta R_{1.5B}$ †	68.4	41.0%	9.5	31.5%	41.5	38.5%	23.0	51.7%	34.6	57.4%	89.8	50.0%
SimpleRL-7B	76.3	-	15.6	-	55.9	-	25.9	-	39.5	-	91.9	-

† indicates that the prompt used for RAST does not match the one used to train the small RL-tuned model (see Figure 7), due to the training inconsistency for available RL-tuned models (e.g., from SimpleRL-Zoo). As a result, the transferred $\Delta R_{1.5B}$ yields relatively smaller gains.

Table 2: Experiment results of RAST on mathematical reasoning datasets. ΔR is borrowed from Llama-3.1-8B-SimpleRL-Zoo [72]. Numbers are computed on 32 runs with sampling.

Models	Math500	AIME24	AMC	Minerva	Olympiad	GSM8K
Llama-3.1-70B	26.2	0.0	12.5	10.3	5.9	56.1
$+\Delta R_{8B}$	33.1	2.8	16.9	12.6	7.1	82.2

Table 3: Experiment results of RAST on code reasoning tasks with the Qwen-2.5-14B-1M model as $\mathcal{M}_{base}$ and ΔR from Code-R1-Zero [39] using greedy decoding.

Models	HumanEval+	MBPP+	LiveCodeBench	Average
Qwen-2.5-14B-1M	82.3	69.6	34.3	62.1
$+\Delta R_{7B}$	85.4	76.5	37.6	66.5

Decoding Configurations To accelerate the inference speed, we implemented a revised vLLM [27] version to support RAST. For mathematical reasoning, decoding is performed using a temperature setting of 1.0 and nucleus sampling with a top-p of 0.95, allowing a maximum generation length of $16,384$ tokens, consistent with prior work [72]. We set λ in Equation 3 to 1.0 for all experiments. For code reasoning tasks, we follow previous evaluation settings [39, 24] and use greedy decoding. Specifically, we use EvalPlus [37, 38] for HumanEval+ and MBPP+. Our experiments are conducted over 8 NVIDIA A6000 GPUs on a single node, with GPU utilization and tensor parallelism parameters dynamically adjusted based on the model size. Typically, inference requires approximately 30 minutes per run for larger datasets like MATH500 and GSM8K, whereas smaller datasets such as AIME24 and AMC23 complete within 3–5 minutes per run. For specific parameters used for each benchmark, please refer to Appendix B.

3.2 Main Results

RAST enables consistent and scalable reasoning gains. Table 1 summarizes the performance of RAST on six mathematical reasoning benchmarks using the Qwen-2.5 model family at 1.5B, 7B, 14B, and 32B scales. Across all settings, RAST delivers substantial improvements over the base models in both averaged pass@1 and the corresponding recovery rate. Notably, with signals from smaller RL-trained models, RAST can even approach or beat the performance of RL-trained counterparts of the base model. For instance, applying ΔR_{14B} to the 32B base model achieves approximate or superior results on MATH500, Minerva, and GSM8K compared with the 32B RL-trained model. These findings validate the effectiveness of RAST in enhancing reasoning capabilities at inference time, without any retraining or RL on the target model.

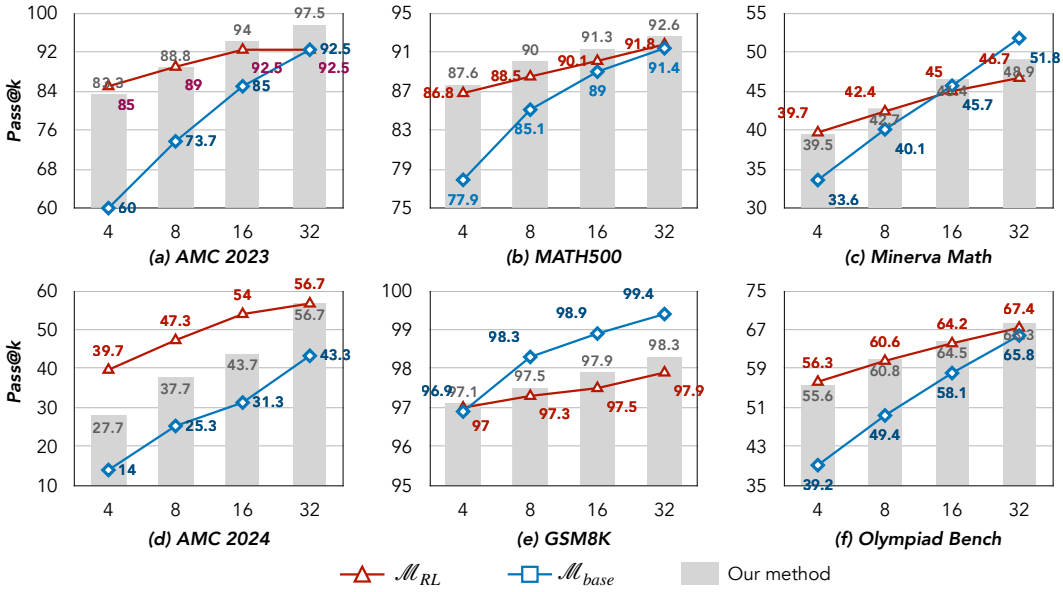

Figure 3: The illustration of pass@k for different values of k on 6 mathematical reasoning datasets, where $\mathcal{M}_{\text{base}}$ is Qwen-2.5-32B, RAST uses ΔR_{14B}, and $\mathcal{M}_{\text{RL}}$ is the RL-trained version of $\mathcal{M}_{\text{base}}$.

ΔR from stronger experts yield greater gains. The effectiveness of RAST also depends on the strength of the $\mathcal{S}_{\text{RL}}$ and $\mathcal{S}_{\text{base}}$ that generates the delta logit ΔR. For each base model, using larger delta sources (e.g., base model of 32B with ΔR_{7B} or ΔR_{14B} compared with $\Delta R_{1.5B}$) leads to greater improvement. Taking the 32B base on MATH500 as an example, accuracy increases progressively from 73.7 (with $\Delta R_{1.5B}$) to 80.7 (with ΔR_{14B}), while the ceiling model, or the upper bound reaches 81.3. Similarly, ΔR_{7B} also works better than $\Delta R_{1.5B}$ for the 14B base model across all datasets. This trend suggests that logit deltas encode richer reasoning signals as the $\mathcal{S}_{RL}$ model scale increases, making RAST a flexible tool for knowledge transfer across various model scales.

Trade-off between $\mathcal{M}_{\text{base}}$ and ΔR. The effectiveness of RAST also depends on the capacity of the base model $\mathcal{M}_{\text{base}}$ and its alignment with ΔR. In general, stronger base models exhibit higher recovery rates, indicating greater receptiveness to transferred reasoning signals. For example, when applying RAST to the 32B base, the recovery rate is often higher than when using 14B or 7B. On GSM8K, RAST bridges nearly the entire gap between the base model (93.1) and the RL expert (95.7), achieving 95.3 with the delta logit from a 14B model. In contrast, for the 7B base, the gain is smaller (87.7 to 91.9), even though the same ΔR_{7B} is applied. This suggests that higher-capacity base models are more receptive to the transferred reasoning signal. However, increasing base model capacity alone does not guarantee better outcomes. When applying ΔR_{7B} to both 14B and 32B bases, the 14B base yields a higher recovery rate, suggesting that a large capability gap between the base and ΔR may hinder effective transfer. These observations highlight a trade-off: while stronger base models benefit more from compatible deltas, excessively mismatched pairs may reduce the efficacy of reasoning activation.

3.3 RAST Boosts Reasoning Diversity

Figure 3 illustrates the pass@k accuracy trends across six mathematical reasoning benchmarks, using the Qwen-2.5-32B base model augmented with ΔR_{14B}. For each problem, we randomly sample k outputs from a 32-sample pool, repeat this process 10 times, and report the average accuracy. This setup allows us to assess how well RAST supports diverse solution trajectories under varying sampling sizes. Based on the results, we have the following key observations:

Increasing k consistently improves accuracy. Across all benchmarks, pass@k increases monotonically with larger k, confirming the benefit of sampling multiple decoding paths. This trend reflects that RAST promotes solution diversity—a larger k enables broader exploration of plausible answers, increasing the likelihood of capturing correct responses even when individual generations are imperfect. We also noticed that on most benchmarks except GSM8K, pass@k for $\mathcal{M}_{\text{RL}}$ is large than $\mathcal{M}_{\text{base}}$, which might result from GSM8K's simplicity.

Pass@k surpasses the ceiling performance. Remarkably, in all benchmarks, RAST achieves pass@k accuracy that equals or even exceeds the performance of $\mathcal{M}_{\text{RL}}$. This stands in contrast to prior findings [54, 70], which reported limited or deteriorated performance in pass@k under RL training. We posit that this effect may stem from the implicit ensembling of knowledge across models, which enhances diversity in the search space. Additionally, RAST can sometimes beat the pass@k of $\mathcal{M}_{\text{base}}$ on benchmarks like AMC, MATH500, and Olympiad Bench. This surprising behavior suggests that RAST not only saves the costly training efforts of RL, but also introduces a distinct form of diversity or guidance in the sampling space that helps recover correct answers, a notable drawback of RL-trained models.

3.4 RAST Generalizes Well to Other Models and Tasks

We conduct experiments of RAST on another model family, Llama-3.1, and on additional code reasoning tasks. The results are shown in Tables 2 and 3. Applying RAST to Llama-3.1-70B using ΔR_{8B} from a smaller RL-tuned model [72] yields consistent gains across all six mathematical reasoning datasets. As shown in Table 2, we observe a $+2.8$ absolute improvement on AIME24, $+4.4$ on AMC, and $+2.3$ on Olympiad. We also found that the improvement in MATH500 and GSM8K was particularly high. This might be due to the training recipe of S_{RL}, where they are trained with problems from MATH500 and GSM8K. Nonetheless, the experiments demonstrate that RAST is effective for different model families apart from Qwen, reaffirming the hypothesis that reasoning-relevant distributional shifts are transferrable and model-agnostic. In Table 3, we evaluate RAST on Qwen-2.5-14B-1M [68] using ΔR from its 7B counterpart [39] on three code reasoning benchmarks. RAST achieves consistent improvements on all datasets, leading to an overall +4.4 absolute improvement in average performance. This indicates that the method is not limited to mathematical reasoning, but code-related reasoning tasks. These findings confirm the broad applicability of RAST across model architectures, parameter scales, and reasoning domains.

4 Understanding Reasoning Activation

4.1 Similarity of ΔR as Signal for Transferability

As shown in Table 1, model performance varies widely across settings, motivating the need to understand what governs effective transferability. The delta logits ΔR (defined in Equation 3) capture the modification induced by the reasoning-enhanced model relative to its base. To quantify the alignment between these delta logits across different model pairs, we adopt *cosine similarity* as the measure. This choice is motivated by prior work [58, 15], which demonstrates that cosine similarity effectively captures directional alignment in high-dimensional spaces, independent of magnitude. Following Section 2, we randomly sample 50 examples from MATH500 and extract the decoding trajectory T (with tokens t) generated by SimpleRL-32B. Each trajectory is then fed through $\mathcal{M}_{\text{base}}$ and $\mathcal{M}_{\text{RL}}$ token by token to compute ΔR with prefix $T_{<t}$. We then log the average cosine similarity across the trajectory as:

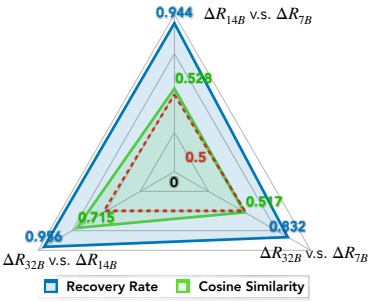

Figure 4: Cosine similarity vs. recovery rate across delta logit pairs (ΔR) from varying model scales. E.g., "ΔR_{14B} v.s. ΔR_{7B}" denotes AvgCosineSim$(\Delta R_{14B}, \Delta R_{7B})$.

$$\text{AvgCosineSim}(\Delta R_1, \Delta R_2) = \frac{1}{T}\sum_{t=1}^{T} \frac{\Delta R_1^{(t)} \cdot \Delta R_2^{(t)}}{\|\Delta R_1^{(t)}\| \, \|\Delta R_2^{(t)}\|} \tag{6}$$

The results are shown in Figure 4. We found that the recovery rate exhibits a positive correlation with cosine similarity—as ΔR between models becomes more aligned, transferability improves.

4.2 Token-Level Behavior Shift

As a preliminary study mentioned in Section 2.1, we reveal that given the decoding path from RL model $\mathcal{M}_{\text{RL}}$, the base model $\mathcal{M}_{\text{base}}$ actually will largely recover the path, with PRC of 95.22% (for 32B model). In this section, we delve deeper into this study. Firstly, we repeat the study using $\tilde{\mathcal{M}}$ tuned by RAST by feeding the decoding path of $\mathcal{M}_{\text{RL}}$ to $\tilde{\mathcal{M}}$. The PRC in this experiment is

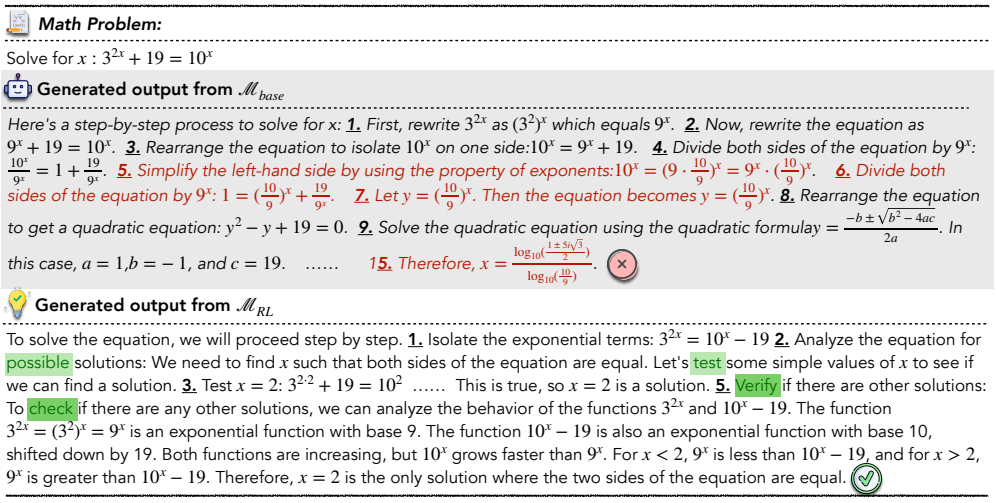

Figure 5: A case study comparing generated outputs for the same math problem sampled from MATH500 from $\mathcal{M}_{\text{base}}$ and $\tilde{\mathcal{M}}$ obtained by RAST. The red denotes erroneous thinking steps from $\mathcal{M}_{\text{base}}$ while the green texts indicate remarkably large KLD, with deeper color denoting larger KLD.

$O_{\tilde{\mathcal{M}}} = 96.37\%$, which is even higher. This phenomenon indicates that RAST provides efficient guidance for the base model $\mathcal{M}_{\text{base}}$ in the search space, echoing the conclusion in [70].

Apart from the overall quantitative view, we also present a more intuitive interpretation in Figure 5. We can see that the generated output from $\mathcal{M}_{\text{base}}$ follows only one thinking and contains many erroneous steps without self-verification. However, the output from $\tilde{\mathcal{M}}$ demonstrates a markedly different reasoning behavior. It first *proposes and tests* a candidate solution, then explicitly *verifies* its correctness, and finally reasons about the function behavior to *rule out other possibilities*. To make it more rigorous, we compute the KL divergence [26] online during inference as $KLD(\mathcal{M}_{\text{base}}(t_i, x_{<i}), \tilde{\mathcal{M}}(t_i, x_{<i}))$ where $x_{<t}$ is the current prefix. Notably, we found that the KLD for tokens such as "check" reaches 837.9, which is far larger than normal tokens that usually stay below 1.0. These behavioral differences underscore the effectiveness of RAST in activating reasoning behaviors. We also provide an additional quantitative analysis for reasoning token behaviors in Appendix C.3.

4.3 Efficiency Analysis

This section presents the efficiency analysis in terms of estimated GPU memory requirements, highlighting the computational advantage of RAST over conventional RL training. We summarize the results in Table 4. We estimate the memory overhead in terms of GPU memory used for RAST (including training $\mathcal{S}_{\text{RL}}$ and inference cost), and $\mathcal{M}_{\text{RL}}$. The results are estimated considering tensor parallel and CPU offloading (since these are common tricks during training) based on the following dimensions: (i) model memory footprint (FP16), (ii) optimizer states, and (iii) activations & buffers. Details of the computation for estimation could be found in Appendix D. Despite using significantly fewer resources, RAST achieves high recovery rates across all settings (e.g., reaching over 84% in the most demanding 32B + ΔR_{14B} configuration). This demonstrates that our method retains most of the performance benefits of full-scale RL training while reducing the computational burden by up to 50% in terms of GPU memory and hardware requirements.

Table 4: Comparison on memory overhead between our approach RAST and the conventional RL training pipeline (i.e., GRPO). We also report the averaged performance recovery rate (RR.) across all mathematical reasoning benchmarks.

Settings	32B		32B		14B	
	$\mathcal{M}_{\text{base}}$	$\mathcal{M}_{\text{RL}}$	$\mathcal{M}_{\text{base}}$	$\mathcal{M}_{\text{RL}}$	$\mathcal{M}_{\text{base}}$	$\mathcal{M}_{\text{RL}}$
	$+\Delta R_{14B}$	-	$+\Delta R_{7B}$	-	$+\Delta R_{7B}$	-
GPU memory	~160G	~350G	~100G	~350G	~100G	~160G
# GPU cards	4×80G	8×80G	2×80G	8×80G	2×80G	4×80G
Averaged RR.	84.8%	100%	63.4%	100%	83.9%	100%

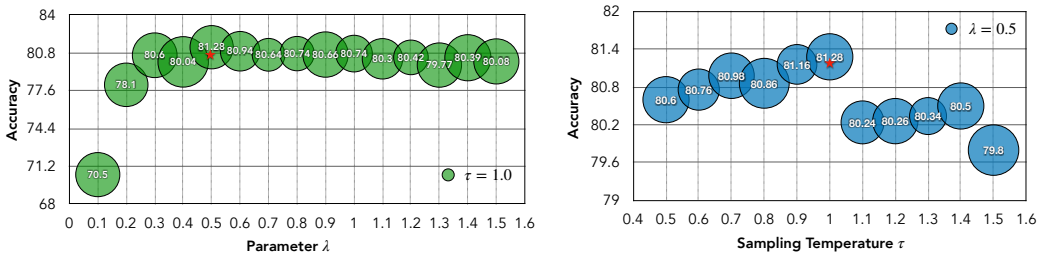

Figure 6: Experiment results with varying λ (left) and τ (right) on MATH500 dataset, ★ denotes the peak performance. The position represents the accuracy, and the size of the circle denotes the standard deviation over 32 runs.

4.4 Robustness regarding τ and λ

To evaluate the sensitivity of our method to decoding-time hyperparameters, we perform a grid search over sampling temperature τ and λ used in Equation 3. The results are summarized with performance trends visualized in Figure 6. We plot accuracy across varying τ values (with $\lambda = 0.5$ fixed) and varying λ values (with $\tau = 1.0$ fixed), including standard deviation error bars to reflect stability across multiple runs. Note that we use these fixed values for investigation since they represent the peak performance. In both settings, the accuracy remains consistently high within a reasonable range. Specifically, with $\tau \in [0.5, 1.0]$ and $\lambda \in [0.3, 1.5]$, the performance would be reasonably good within a certain range. These trends demonstrate that our method is robust to moderate fluctuations in decoding-time hyperparameters and does not rely on precise tuning for strong performance.

5 Related Work

5.1 Reinforcement Learning for LLM Complex Reasoning

Reinforcement learning (RL) has emerged as an important process of LLM post-training for human preference alignment. Early successes such as reinforcement learning with human feedback (RLHF) [47] demonstrated the effectiveness of reward modeling from preference data [71, 7]. Building upon this, follow-up works have explored RL as a means to directly optimize for reasoning quality [23] with outcome supervision [28] or process supervision [32, 61] as verifiable rewards, specifically in the domain of math [54] and coding [63, 39].

More recently, the success of DeepSeek-R1 [14] introduced a notable shift in training methodology with the "zero-RL" paradigm, where RL is applied directly to the base LLM, entirely bypassing intermediate supervised fine-tuning. Following its release, the open-source community has made significant strides in replicating [72, 48, 77], extending [69], and interpreting [74, 70, 41] the R1 algorithm and its behavioral consequences. Our work builds directly upon these open-source Zero-RL models and takes a step further by exploring whether the reasoning behaviors elicited through RL in small models can be transferred to larger base models without additional RL training. Specifically, we focus on leveraging the output distribution (logits) of small RL-trained reasoning models to activate similar behaviors in larger models across scales.

5.2 Decoding-time Strategy for Reasoning Enhancement

Decoding-time methods [56] have been explored largely in text generation, typically by manipulating the logit distribution from base language models. Earlier research efforts focused on sampling-based strategies aimed at improving generation quality through techniques like hierarchical decoding [10], nucleus sampling [20], and locally typical sampling [44]. More recent approaches incorporate the notion of *contrastiveness* [30, 36], which exploits the disagreement between a stronger (expert) and a weaker (amateur) model to downweight completions favored by the weaker model. These contrastive methods have shown effectiveness in improving factuality, diversity, and coherence in open-ended generation [35, 5, 45]. The contrastive decoding framework has since been extended to a variety of downstream tasks, including machine translation [62], retrieval-augmented generation (RAG) [51], and conflict resolution in knowledge-intensive tasks [57].

When it comes to reasoning, [46] explores contrastive decoding for mathematical reasoning, while [34] identifies critical tokens in the reasoning trajectory using contrastive estimation. Our work builds on this growing line of decoding-time reasoning enhancement. Specifically, we leverage the divergence between Zero-RL-trained experts and their base counterparts to guide decoding, aiming to surface and amplify reasoning behaviors. In contrast to prior approaches that operate on instruction-tuned or supervised models, our method explicitly targets RL-induced reasoning signals and explores their transferability across model scales.

6 Conclusion and Discussion

We introduce RAST, a decoding-time framework that enables scalable reasoning enhancement in LLMs by transferring logit-level guidance from smaller RL-tuned models. Comprehensive experiments show that RAST consistently boosts the performance, often approaching or surpassing the performance of much more expensive ceiling models. Further analysis confirms the robustness of our method across decoding hyperparameters and highlights the alignment between delta signals and reasoning activation. Our findings suggest a practical and efficient pathway for eliciting complex reasoning in LLMs, opening new avenues for decoding-time reasoning enhancement and model behavior study for RL. We also present some insights toward future directions in Appendix E.

Acknowledgments and Disclosure of Funding

Research was supported in part by US DARPA INCAS Program No. HR0011-21-C0165 and BRIES Program No. HR0011-24-3-0325, National Science Foundation IIS-19-56151, the Molecule Maker Lab Institute: An AI Research Institutes program supported by NSF under Award No. 2019897, and the Institute for Geospatial Understanding through an Integrative Discovery Environment (I-GUIDE) by NSF under Award No. 2118329. Any opinions, findings, and conclusions or recommendations expressed herein are those of the authors and do not necessarily represent the views, either expressed or implied, of DARPA or the U.S. Government. This research used the DeltaAI advanced computing and data resource, which is supported by the National Science Foundation (award OAC 2320345) and the State of Illinois. DeltaAI is a joint effort of the University of Illinois Urbana-Champaign and its National Center for Supercomputing Applications.

References

[1] Jacob Austin, Augustus Odena, Maxwell Nye, Maarten Bosma, Henryk Michalewski, David Dohan, Ellen Jiang, Carrie Cai, Michael Terry, Quoc Le, et al. Program synthesis with large language models. *arXiv preprint arXiv:2108.07732*, 2021.

[2] Mark Chen, Jerry Tworek, Heewoo Jun, Qiming Yuan, Henrique Ponde de Oliveira Pinto, Jared Kaplan, Harri Edwards, Yuri Burda, Nicholas Joseph, Greg Brockman, Alex Ray, Raul Puri, Gretchen Krueger, Michael Petrov, Heidy Khlaaf, Girish Sastry, Pamela Mishkin, Brooke Chan, Scott Gray, Nick Ryder, Mikhail Pavlov, Alethea Power, Lukasz Kaiser, Mohammad Bavarian, Clemens Winter, Philippe Tillet, Felipe Petroski Such, Dave Cummings, Matthias Plappert, Fotios Chantzis, Elizabeth Barnes, Ariel Herbert-Voss, William Hebgen Guss, Alex Nichol, Alex Paino, Nikolas Tezak, Jie Tang, Igor Babuschkin, Suchir Balaji, Shantanu Jain, William Saunders, Christopher Hesse, Andrew N. Carr, Jan Leike, Josh Achiam, Vedant Misra, Evan Morikawa, Alec Radford, Matthew Knight, Miles Brundage, Mira Murati, Katie Mayer, Peter Welinder, Bob McGrew, Dario Amodei, Sam McCandlish, Ilya Sutskever, and Wojciech Zaremba. Evaluating large language models trained on code. 2021.

[3] Xingyu Chen, Jiahao Xu, Tian Liang, Zhiwei He, Jianhui Pang, Dian Yu, Linfeng Song, Qiuzhi Liu, Mengfei Zhou, Zhuosheng Zhang, et al. Do not think that much for 2+ 3=? on the overthinking of o1-like llms. *arXiv preprint arXiv:2412.21187*, 2024.

[4] Tianzhe Chu, Yuexiang Zhai, Jihan Yang, Shengbang Tong, Saining Xie, Sergey Levine, and Yi Ma. SFT memorizes, RL generalizes: A comparative study of foundation model post-training. In *The Second Conference on Parsimony and Learning (Recent Spotlight Track)*, 2025.

[5] Yung-Sung Chuang, Yujia Xie, Hongyin Luo, Yoon Kim, James R. Glass, and Pengcheng He. Dola: Decoding by contrasting layers improves factuality in large language models. In *The Twelfth International Conference on Learning Representations*, 2024.

[6] Karl Cobbe, Vineet Kosaraju, Mohammad Bavarian, Mark Chen, Heewoo Jun, Lukasz Kaiser, Matthias Plappert, Jerry Tworek, Jacob Hilton, Reiichiro Nakano, et al. Training verifiers to solve math word problems. *arXiv preprint arXiv:2110.14168*, 2021.

[7] Ganqu Cui, Lifan Yuan, Ning Ding, Guanming Yao, Wei Zhu, Yuan Ni, Guotong Xie, Zhiyuan Liu, and Maosong Sun. Ultrafeedback: Boosting language models with high-quality feedback, 2024.

[8] Xingyu Dang, Christina Baek, J Zico Kolter, and Aditi Raghunathan. Assessing diversity collapse in reasoning. In *Scaling Self-Improving Foundation Models without Human Supervision*, 2025.

[9] Thomas G. Dietterich. Ensemble methods in machine learning. In *Proceedings of the First International Workshop on Multiple Classifier Systems*, MCS '00, page 1–15, Berlin, Heidelberg, 2000. Springer-Verlag.

[10] Angela Fan, Mike Lewis, and Yann Dauphin. Hierarchical neural story generation. In Iryna Gurevych and Yusuke Miyao, editors, *Proceedings of the 56th Annual Meeting of the Association for Computational Linguistics (Volume 1: Long Papers)*, pages 889–898, Melbourne, Australia, July 2018. Association for Computational Linguistics.

[11] Kanishk Gandhi, Ayush Chakravarthy, Anikait Singh, Nathan Lile, and Noah D Goodman. Cognitive behaviors that enable self-improving reasoners, or, four habits of highly effective stars. *arXiv preprint arXiv:2503.01307*, 2025.

[12] TNG Technology Consulting GmbH. Deepseek-r1t-chimera, April 2025.

[13] Aaron Grattafiori, Abhimanyu Dubey, Abhinav Jauhri, Abhinav Pandey, Abhishek Kadian, Ahmad Al-Dahle, Aiesha Letman, Akhil Mathur, Alan Schelten, Alex Vaughan, et al. The llama 3 herd of models. *arXiv preprint arXiv:2407.21783*, 2024.

[14] Daya Guo, Dejian Yang, Haowei Zhang, Junxiao Song, Ruoyu Zhang, Runxin Xu, Qihao Zhu, Shirong Ma, Peiyi Wang, Xiao Bi, et al. Deepseek-r1: Incentivizing reasoning capability in llms via reinforcement learning. *arXiv preprint arXiv:2501.12948*, 2025.

[15] Gyeongdo Ham, Seonghak Kim, Suin Lee, Jae-Hyeok Lee, and Daeshik Kim. Cosine similarity knowledge distillation for individual class information transfer. *arXiv preprint arXiv:2311.14307*, 2023.

[16] Alex Havrilla, Yuqing Du, Sharath Chandra Raparthy, Christoforos Nalmpantis, Jane Dwivedi-Yu, Maksym Zhuravinskyi, Eric Hambro, Sainbayar Sukhbaatar, and Roberta Raileanu. Teaching large language models to reason with reinforcement learning. *arXiv preprint arXiv:2403.04642*, 2024.

[17] Chaoqun He, Renjie Luo, Yuzhuo Bai, Shengding Hu, Zhen Thai, Junhao Shen, Jinyi Hu, Xu Han, Yujie Huang, Yuxiang Zhang, Jie Liu, Lei Qi, Zhiyuan Liu, and Maosong Sun. OlympiadBench: A challenging benchmark for promoting AGI with olympiad-level bilingual multimodal scientific problems. In Lun-Wei Ku, Andre Martins, and Vivek Srikumar, editors, *Proceedings of the 62nd Annual Meeting of the Association for Computational Linguistics (Volume 1: Long Papers)*, pages 3828–3850, Bangkok, Thailand, August 2024. Association for Computational Linguistics.

[18] Dan Hendrycks, Collin Burns, Saurav Kadavath, Akul Arora, Steven Basart, Eric Tang, Dawn Song, and Jacob Steinhardt. Measuring mathematical problem solving with the MATH dataset. In *Thirty-fifth Conference on Neural Information Processing Systems Datasets and Benchmarks Track (Round 2)*, 2021.

[19] Andreas Hochlehnert, Hardik Bhatnagar, Vishaal Udandarao, Samuel Albanie, Ameya Prabhu, and Matthias Bethge. A sober look at progress in language model reasoning: Pitfalls and paths to reproducibility. *arXiv preprint arXiv:2504.07086*, 2025.

[20] Ari Holtzman, Jan Buys, Li Du, Maxwell Forbes, and Yejin Choi. The curious case of neural text degeneration. In *International Conference on Learning Representations*, 2020.

[21] Edward J Hu, yelong shen, Phillip Wallis, Zeyuan Allen-Zhu, Yuanzhi Li, Shean Wang, Lu Wang, and Weizhu Chen. LoRA: Low-rank adaptation of large language models. In *International Conference on Learning Representations*, 2022.

[22] Chengsong Huang, Qian Liu, Bill Yuchen Lin, Tianyu Pang, Chao Du, and Min Lin. Lorahub: Efficient cross-task generalization via dynamic loRA composition. In *First Conference on Language Modeling*, 2024.

[23] Aaron Jaech, Adam Kalai, Adam Lerer, Adam Richardson, Ahmed El-Kishky, Aiden Low, Alec Helyar, Aleksander Madry, Alex Beutel, Alex Carney, et al. Openai o1 system card. *arXiv preprint arXiv:2412.16720*, 2024.

[24] Naman Jain, King Han, Alex Gu, Wen-Ding Li, Fanjia Yan, Tianjun Zhang, Sida Wang, Armando Solar-Lezama, Koushik Sen, and Ion Stoica. Livecodebench: Holistic and contamination free evaluation of large language models for code. In *The Thirteenth International Conference on Learning Representations*, 2025.

[25] Leslie Pack Kaelbling, Michael L Littman, and Andrew W Moore. Reinforcement learning: A survey. *Journal of artificial intelligence research*, 4:237–285, 1996.

[26] Solomon Kullback and Richard A Leibler. On information and sufficiency. *The annals of mathematical statistics*, 22(1):79–86, 1951.

[27] Woosuk Kwon, Zhuohan Li, Siyuan Zhuang, Ying Sheng, Lianmin Zheng, Cody Hao Yu, Joseph E. Gonzalez, Hao Zhang, and Ion Stoica. Efficient memory management for large language model serving with pagedattention. In *Proceedings of the ACM SIGOPS 29th Symposium on Operating Systems Principles*, 2023.

[28] Nathan Lambert, Jacob Morrison, Valentina Pyatkin, Shengyi Huang, Hamish Ivison, Faeze Brahman, Lester James V Miranda, Alisa Liu, Nouha Dziri, Shane Lyu, et al. T\" ulu 3: Pushing frontiers in open language model post-training. *arXiv preprint arXiv:2411.15124*, 2024.

[29] Aitor Lewkowycz, Anders Johan Andreassen, David Dohan, Ethan Dyer, Henryk Michalewski, Vinay Venkatesh Ramasesh, Ambrose Slone, Cem Anil, Imanol Schlag, Theo Gutman-Solo, Yuhuai Wu, Behnam Neyshabur, Guy Gur-Ari, and Vedant Misra. Solving quantitative reasoning problems with language models. In Alice H. Oh, Alekh Agarwal, Danielle Belgrave, and Kyunghyun Cho, editors, *Advances in Neural Information Processing Systems*, 2022.

[30] Xiang Lisa Li, Ari Holtzman, Daniel Fried, Percy Liang, Jason Eisner, Tatsunori Hashimoto, Luke Zettlemoyer, and Mike Lewis. Contrastive decoding: Open-ended text generation as optimization. In Anna Rogers, Jordan Boyd-Graber, and Naoaki Okazaki, editors, *Proceedings of the 61st Annual Meeting of the Association for Computational Linguistics (Volume 1: Long Papers)*, pages 12286–12312, Toronto, Canada, July 2023. Association for Computational Linguistics.

[31] Eric Liang, Zhanghao Wu, Michael Luo, Sven Mika, Joseph E. Gonzalez, and Ion Stoica. RLlib flow: Distributed reinforcement learning is a dataflow problem. In A. Beygelzimer, Y. Dauphin, P. Liang, and J. Wortman Vaughan, editors, *Advances in Neural Information Processing Systems*, 2021.

[32] Hunter Lightman, Vineet Kosaraju, Yuri Burda, Harrison Edwards, Bowen Baker, Teddy Lee, Jan Leike, John Schulman, Ilya Sutskever, and Karl Cobbe. Let's verify step by step. In *The Twelfth International Conference on Learning Representations*, 2024.

[33] Bill Yuchen Lin, Abhilasha Ravichander, Ximing Lu, Nouha Dziri, Melanie Sclar, Khyathi Raghavi Chandu, Chandra Bhagavatula, and Yejin Choi. The unlocking spell on base llms: Rethinking alignment via in-context learning. In *The Twelfth International Conference on Learning Representations, ICLR 2024, Vienna, Austria, May 7-11, 2024*. OpenReview.net, 2024.

[34] Zicheng Lin, Tian Liang, Jiahao Xu, Xing Wang, Ruilin Luo, Chufan Shi, Siheng Li, Yujiu Yang, and Zhaopeng Tu. Critical tokens matter: Token-level contrastive estimation enhence llm's reasoning capability. *arXiv preprint arXiv:2411.19943*, 2024.

[35] Alisa Liu, Xiaochuang Han, Yizhong Wang, Yulia Tsvetkov, Yejin Choi, and Noah A. Smith. Tuning language models by proxy. In *First Conference on Language Modeling*, 2024.

[36] Alisa Liu, Maarten Sap, Ximing Lu, Swabha Swayamdipta, Chandra Bhagavatula, Noah A. Smith, and Yejin Choi. DExperts: Decoding-time controlled text generation with experts and anti-experts. In Chengqing Zong, Fei Xia, Wenjie Li, and Roberto Navigli, editors, *Proceedings of the 59th Annual Meeting of the Association for Computational Linguistics and the 11th International Joint Conference on Natural Language Processing (Volume 1: Long Papers)*, pages 6691–6706, Online, August 2021. Association for Computational Linguistics.

[37] Jiawei Liu, Chunqiu Steven Xia, Yuyao Wang, and Lingming Zhang. Is your code generated by chatGPT really correct? rigorous evaluation of large language models for code generation. In *Thirty-seventh Conference on Neural Information Processing Systems*, 2023.

[38] Jiawei Liu, Songrun Xie, Junhao Wang, Yuxiang Wei, Yifeng Ding, and Lingming Zhang. Evaluating language models for efficient code generation. In *First Conference on Language Modeling*, 2024.

[39] Jiawei Liu and Lingming Zhang. Code-r1: Reproducing r1 for code with reliable rewards. 2025.

[40] Zichen Liu, Changyu Chen, Wenjun Li, Tianyu Pang, Chao Du, and Min Lin. There may not be aha moment in r1-zero-like training — a pilot study. https://oatllm.notion.site/oat-zero, 2025. Notion Blog.

[41] Zichen Liu, Changyu Chen, Wenjun Li, Penghui Qi, Tianyu Pang, Chao Du, Wee Sun Lee, and Min Lin. Understanding r1-zero-like training: A critical perspective. *arXiv preprint arXiv:2503.20783*, 2025.

[42] Xinyin Ma, Guangnian Wan, Runpeng Yu, Gongfan Fang, and Xinchao Wang. Cot-valve: Length-compressible chain-of-thought tuning. *arXiv preprint arXiv:2502.09601*, 2025.

[43] Sara Vera Marjanović, Arkil Patel, Vaibhav Adlakha, Milad Aghajohari, Parishad BehnamGhader, Mehar Bhatia, Aditi Khandelwal, Austin Kraft, Benno Krojer, Xing Han Lù, et al. Deepseek-r1 thoughtology: Let's< think> about llm reasoning. *arXiv preprint arXiv:2504.07128*, 2025.

[44] Clara Meister, Tiago Pimentel, Gian Wiher, and Ryan Cotterell. Locally typical sampling. *Transactions of the Association for Computational Linguistics*, 11:102–121, 2023.

[45] Eric Mitchell, Rafael Rafailov, Archit Sharma, Chelsea Finn, and Christopher D Manning. An emulator for fine-tuning large language models using small language models. In *The Twelfth International Conference on Learning Representations*, 2024.

[46] Sean O'Brien and Mike Lewis. Contrastive decoding improves reasoning in large language models. *arXiv preprint arXiv:2309.09117*, 2023.

[47] Long Ouyang, Jeff Wu, Xu Jiang, Diogo Almeida, Carroll L. Wainwright, Pamela Mishkin, Chong Zhang, Sandhini Agarwal, Katarina Slama, Alex Ray, John Schulman, Jacob Hilton, Fraser Kelton, Luke Miller, Maddie Simens, Amanda Askell, Peter Welinder, Paul Christiano, Jan Leike, and Ryan Lowe. Training language models to follow instructions with human feedback. In *Proceedings of the 36th International Conference on Neural Information Processing Systems*, NIPS '22, Red Hook, NY, USA, 2022. Curran Associates Inc.

[48] Jiayi Pan, Junjie Zhang, Xingyao Wang, Lifan Yuan, Hao Peng, and Alane Suhr. Tinyzero. https://github.com/Jiayi-Pan/TinyZero, 2025. Accessed: 2025-01-24.

[49] Richard Yuanzhe Pang, Weizhe Yuan, He He, Kyunghyun Cho, Sainbayar Sukhbaatar, and Jason Weston. Iterative reasoning preference optimization. *Advances in Neural Information Processing Systems*, 37:116617–116637, 2024.

[50] Tian Qin, David Alvarez-Melis, Samy Jelassi, and Eran Malach. To backtrack or not to backtrack: When sequential search limits model reasoning. *arXiv preprint arXiv:2504.07052*, 2025.

[51] Zexuan Qiu, Zijing Ou, Bin Wu, Jingjing Li, Aiwei Liu, and Irwin King. Entropy-based decoding for retrieval-augmented large language models. 2025.

[52] John Schulman, Filip Wolski, Prafulla Dhariwal, Alec Radford, and Oleg Klimov. Proximal policy optimization algorithms. *arXiv preprint arXiv:1707.06347*, 2017.

[53] Amrith Setlur, Chirag Nagpal, Adam Fisch, Xinyang Geng, Jacob Eisenstein, Rishabh Agarwal, Alekh Agarwal, Jonathan Berant, and Aviral Kumar. Rewarding progress: Scaling automated process verifiers for LLM reasoning. In *The Thirteenth International Conference on Learning Representations*, 2025.

[54] Zhihong Shao, Peiyi Wang, Qihao Zhu, Runxin Xu, Junxiao Song, Mingchuan Zhang, Y.K. Li, Y. Wu, and Daya Guo. Deepseekmath: Pushing the limits of mathematical reasoning in open language models, 2024.

[55] Guangming Sheng, Chi Zhang, Zilingfeng Ye, Xibin Wu, Wang Zhang, Ru Zhang, Yanghua Peng, Haibin Lin, and Chuan Wu. Hybridflow: A flexible and efficient RLHF framework. In *Proceedings of the Twentieth European Conference on Computer Systems, EuroSys 2025, Rotterdam, The Netherlands, 30 March 2025 - 3 April 2025*, pages 1279–1297. ACM, 2025.

[56] Chufan Shi, Haoran Yang, Deng Cai, Zhisong Zhang, Yifan Wang, Yujiu Yang, and Wai Lam. A thorough examination of decoding methods in the era of LLMs. In Yaser Al-Onaizan, Mohit Bansal, and Yun-Nung Chen, editors, *Proceedings of the 2024 Conference on Empirical Methods in Natural Language Processing*, pages 8601–8629, Miami, Florida, USA, November 2024. Association for Computational Linguistics.

[57] Weijia Shi, Xiaochuang Han, Mike Lewis, Yulia Tsvetkov, Luke Zettlemoyer, and Wen-tau Yih. Trusting your evidence: Hallucinate less with context-aware decoding. In Kevin Duh, Helena Gomez, and Steven Bethard, editors, *Proceedings of the 2024 Conference of the North American Chapter of the Association for Computational Linguistics: Human Language Technologies (Volume 2: Short Papers)*, pages 783–791, Mexico City, Mexico, June 2024. Association for Computational Linguistics.

[58] Sungho Shin, Joosoon Lee, Junseok Lee, Yeonguk Yu, and Kyoobin Lee. Teaching where to look: Attention similarity knowledge distillation for low resolution face recognition. In *Computer Vision – ECCV 2022*, pages 631–647, Cham, 2022. Springer Nature Switzerland.

[59] Richard S Sutton, Andrew G Barto, et al. *Reinforcement learning: An introduction*, volume 1. MIT press Cambridge, 1998.

[60] Gokul Swamy, Sanjiban Choudhury, Wen Sun, Zhiwei Steven Wu, and J Andrew Bagnell. All roads lead to likelihood: The value of reinforcement learning in fine-tuning. *arXiv preprint arXiv:2503.01067*, 2025.

[61] Luong Trung, Xinbo Zhang, Zhanming Jie, Peng Sun, Xiaoran Jin, and Hang Li. ReFT: Reasoning with reinforced fine-tuning. In Lun-Wei Ku, Andre Martins, and Vivek Srikumar, editors, *Proceedings of the 62nd Annual Meeting of the Association for Computational Linguistics (Volume 1: Long Papers)*, pages 7601–7614, Bangkok, Thailand, August 2024. Association for Computational Linguistics.

[62] Jonas Waldendorf, Barry Haddow, and Alexandra Birch. Contrastive decoding reduces hallucinations in large multilingual machine translation models. In Yvette Graham and Matthew Purver, editors, *Proceedings of the 18th Conference of the European Chapter of the Association for Computational Linguistics (Volume 1: Long Papers)*, pages 2526–2539, St. Julian's, Malta, March 2024. Association for Computational Linguistics.

[63] Junqiao Wang, Zeng Zhang, Yangfan He, Yuyang Song, Tianyu Shi, Yuchen Li, Hengyuan Xu, Kunyu Wu, Guangwu Qian, Qiuwu Chen, et al. Enhancing code llms with reinforcement learning in code generation. *arXiv preprint arXiv:2412.20367*, 2024.

[64] Yuyang Wu, Yifei Wang, Tianqi Du, Stefanie Jegelka, and Yisen Wang. When more is less: Understanding chain-of-thought length in llms. *arXiv preprint arXiv:2502.07266*, 2025.

[65] Heming Xia, Yongqi Li, Chak Tou Leong, Wenjie Wang, and Wenjie Li. Tokenskip: Controllable chain-of-thought compression in llms, 2025.

[66] Tian Xie, Zitian Gao, Qingnan Ren, Haoming Luo, Yuqian Hong, Bryan Dai, Joey Zhou, Kai Qiu, Zhirong Wu, and Chong Luo. Logic-rl: Unleashing llm reasoning with rule-based reinforcement learning. *arXiv preprint arXiv:2502.14768*, 2025.

[67] An Yang, Baosong Yang, Beichen Zhang, Binyuan Hui, Bo Zheng, Bowen Yu, Chengyuan Li, Dayiheng Liu, Fei Huang, Haoran Wei, et al. Qwen2. 5 technical report. *arXiv preprint arXiv:2412.15115*, 2024.

[68] An Yang, Bowen Yu, Chengyuan Li, Dayiheng Liu, Fei Huang, Haoyan Huang, Jiandong Jiang, Jianhong Tu, Jianwei Zhang, Jingren Zhou, et al. Qwen2. 5-1m technical report. *arXiv preprint arXiv:2501.15383*, 2025.

[69] Qiying Yu, Zheng Zhang, Ruofei Zhu, Yufeng Yuan, Xiaochen Zuo, Yu Yue, Tiantian Fan, Gaohong Liu, Lingjun Liu, Xin Liu, et al. Dapo: An open-source llm reinforcement learning system at scale. *arXiv preprint arXiv:2503.14476*, 2025.

[70] Yang Yue, Zhiqi Chen, Rui Lu, Andrew Zhao, Zhaokai Wang, Shiji Song, and Gao Huang. Does reinforcement learning really incentivize reasoning capacity in llms beyond the base model? *arXiv preprint arXiv:2504.13837*, 2025.

[71] Huaye Zeng, Dongfu Jiang, Haozhe Wang, Ping Nie, Xiaotong Chen, and Wenhu Chen. Acecoder: Acing coder rl via automated test-case synthesis. *arXiv preprint arXiv:2502.01718*, 2025.

[72] Weihao Zeng, Yuzhen Huang, Qian Liu, Wei Liu, Keqing He, Zejun Ma, and Junxian He. Simplerl-zoo: Investigating and taming zero reinforcement learning for open base models in the wild. *arXiv preprint arXiv:2503.18892*, 2025.

[73] Jinghan Zhang, Xiting Wang, Fengran Mo, Yeyang Zhou, Wanfu Gao, and Kunpeng Liu. Entropy-based exploration conduction for multi-step reasoning. *arXiv preprint arXiv:2503.15848*, 2025.

[74] Rosie Zhao, Alexandru Meterez, Sham Kakade, Cengiz Pehlevan, Samy Jelassi, and Eran Malach. Echo chamber: Rl post-training amplifies behaviors learned in pretraining. *arXiv preprint arXiv:2504.07912*, 2025.

[75] Yaowei Zheng, Junting Lu, Shenzhi Wang, Zhangchi Feng, Dongdong Kuang, and Yuwen Xiong. Easyr1: An efficient, scalable, multi-modality rl training framework. https://github.com/hiyouga/EasyR1, 2025.

[76] Ming Zhong, Chenxin An, Weizhu Chen, Jiawei Han, and Pengcheng He. Seeking neural nuggets: Knowledge transfer in large language models from a parametric perspective. In *The Twelfth International Conference on Learning Representations*, 2024.

[77] Hengguang Zhou, Xirui Li, Ruochen Wang, Minhao Cheng, Tianyi Zhou, and Cho-Jui Hsieh. R1-zero's" aha moment" in visual reasoning on a 2b non-sft model. *arXiv preprint arXiv:2503.05132*, 2025.

A Implementation Details

A.1 Datasets

We provide the details for all the datasets used in our work as follows. All datasets or benchmarks used in this paper are publicly available online. For mathematical reasoning tasks, we include 6 widely used datasets, detailed below:

MATH500 The original MATH collection contains 12,500 problems in total, with 8,000 training and 4,500 test problems, meticulously curated to cover a wide range of topics and difficulty levels. Each problem in MATH has a full step-by-step solution that can be used to teach models to generate answer derivations and explanations. MATH500 (could be found at https://huggingface.co/datasets/HuggingFaceH4/MATH-500) is a non-standard train/test split of the original MATH dataset [18], following [32] to avoid the risk of over-fitting and for more efficient testing configurations. These 500 test problems are selected uniformly at random, and are representative of the test set as a whole.

GSM8K GSM8K (Grade School Math 8K) [6] is a dataset of 8,500 high-quality linguistically diverse grade school math word problems. The dataset was created to support the task of question answering on basic mathematical problems that require multi-step reasoning. The test set of GSM8K (could be found at https://huggingface.co/datasets/openai/gsm8k) includes 1,319 problems in total.

Olympiad Bench Olympiad Bench [17] is originally an Olympiad-level bilingual multimodal scientific benchmark, which contains 8,952 math and physics questions from international Olympiads, Chinese Olympiads, Chinese college entrance examinations, and mock exams. To support our testing needs, we select a subset from the Olympiad Bench that is categorized as "open-ended", "text-only" and "competition-level". Together, there are 675 test problems (could be found at https://huggingface.co/datasets/Hothan/OlympiadBench/viewer/OE_TO_maths_en_COMP) for this subset used in our paper.

AIME The collection of AIME actually contains problems from the American Invitational Mathematics Examination (AIME). AIME is a prestigious high school mathematics competition known for its challenging mathematical problems. In our work, we follow previous works and adopt all the 30 problems (could be found at https://huggingface.co/datasets/HuggingFaceH4/aime_2024) in AIME 2024 for testing purposes.

AMC Similar to AIME, AMC is another very challenging dataset that contain problems in competitions, specifically, the American Mathematics Competitions (AMC). The collection of AMC actually contains 40 problems (could be found at https://huggingface.co/datasets/math-ai/amc23) in total in the year of 2023 for our testing set.

Minerva The testing set of Minerva math is curated in [29], which consists of STEM problems at the undergraduate level. In total, there are 272 problems (could be found at https://huggingface.co/datasets/math-ai/minervamath), 191 of which have numeric solutions and 81 have symbolic solutions.

For code reasoning tasks, we incorporate three datasets as following:

HumanEval+ HumanEval+ is an adapted version from the original HumanEval by [37]. HumanEval+ extends beyond HumanEval with additional high-quality and automatically generated test inputs to 80×, powered by both LLM- and mutation-based strategies. It contains 164 samples for testing (could be found at https://huggingface.co/datasets/evalplus/humanevalplus).

MBPP+ HumanEval+ is also an adapted version from the original MBPP by [37]. The construction process is quite similar to HumanEval+, and it contains 378 samples for the testset (could be found at https://huggingface.co/datasets/evalplus/mbppplus).

Prompt (a)

<lim_startl>**system**
You are a helpful assistant.<lim_endl>
<lim_startl>**user**
{input}
Please reason step by step, and put your final answer within \\boxed{{}}.<lim_endl>
<lim_startl>assistant

Prompt (b)

Question:\n*{input}*\n**Answer:**\nLet's think step by step.

Figure 7: Prompt templates used for mathematical reasoning tasks.

Table 5: Detailed decoding configurations (hyperparameters) used in our experiments.

Settings	gpu_utilization	tensor_parallel_size	temperature	λ	top_p	max_seq_len
Qwen-2.5-32B	0.6	4	0.0	1.0	1.0	16,384
+$\Delta R_{1.5B}$	0.6	4	1.0	1.0	0.95	
+ΔR_{7B}	0.75	4				
+ΔR_{14B}	0.75	4				
32B-RLZero	0.6	4				
Qwen-2.5-14B	0.6	2	0.0	1.0	1.0	16,384
+$\Delta R_{1.5B}$	0.6	2	1.0	1.0	0.95	
+ΔR_{7B}	0.75	2				
14B-RLZero	0.6	2				
Qwen-2.5-7B	0.6	1	0.0	1.0	1.0	16,384
+$\Delta R_{1.5B}$	0.6	1	1.0	1.0	0.95	
7B-RLZero	0.6	1				

LiveCodeBench LiveCodeBench [24] is a recently proposed benchmark that aims at a comprehensive and contamination-free evaluation of LLMs for code, which continuously collects new problems over time from contests across three competition platforms, namely LeetCode, AtCoder, and CodeForces. In our experiments, there are 880 test samples in total.

A.2 Prompt Templates for Inference

Inference prompts used in this work generally following the common practice in the open-source community. Specifically for mathematical reasoning tasks, there are two kinds of prompts as shown in Figure 7. During our experiments, we select experiments with respect to ΔR. For $\Delta R_{1.5B}$, we choose to use *Prompt (b)* following the training and inference setting in [72] since the model scale is too small to follow the complex chat template and output format instruction of "\boxed". For both prompt templates, the "{input}" will be substituted with the corresponding input problem for each data sample.

B Decoding Configurations

Table 5 presents the detailed decoding configurations for our experiments, specifically, the hyperparameters used.

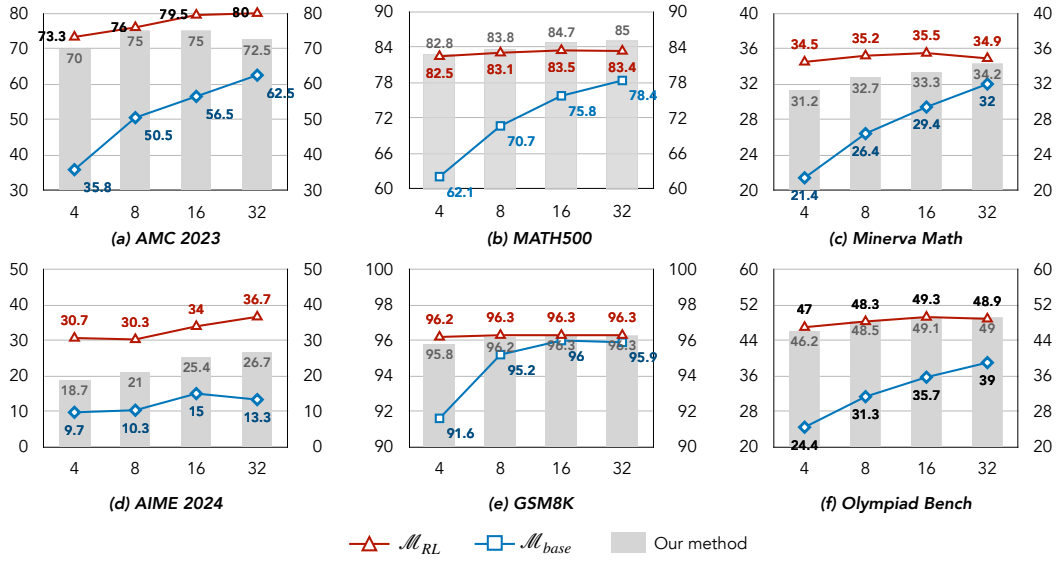

Figure 8: The illustration of majority@k for different values of k on 6 mathematical reasoning datasets, where $\mathcal{M}_{base}$ is Qwen-2.5-32B, RAST uses ΔR_{14B}, and $\mathcal{M}_{Rl}$ is the Rl-trained version of $\mathcal{M}_{base}$.

C More Results

C.1 Performance of Majority@k

We first introduce an additional metric for this additional evaluation.

Definition of Majority@k: This metric evaluates accuracy based on the majority prediction among multiple inference runs per problem. Formally,

$$\text{Majority@k} = \frac{1}{N}\sum_{i=1}^{N}\mathbb{I}\left(\text{majority}\{\hat{y}_{i,1},\hat{y}_{i,2},\ldots,\hat{y}_{i,k}\} = y_i\right),$$

where the majority function returns the prediction most frequently appearing among the k inference runs for the i-th problem. Compared with **Pass@k** that represents diversity, the metric of majority@k reflects the robustness and consistency of the model performance.

We visualize the results in Figure 8, showing the progression of majority@k as k increases across six mathematical reasoning benchmarks. As expected, majority@k improves monotonically with larger k, reflecting the benefit of aggregating more diverse sampled trajectories. In most cases, our method (gray bars) bridges a significant portion of the performance gap between the base model $\mathcal{M}base$ (blue line) and the RL-trained model $\mathcal{M}RL$ (red line), particularly on datasets like MATH500 and GSM8K, where our approach nearly saturates the performance ceiling. This suggests strong consistency among sampled outputs and robust transfer of reasoning behaviors.

In contrast, on more challenging datasets such as AIME 2024 and AMC 2023, a wider gap remains between RAST and $\mathcal{M}_{RL}$, indicating that these tasks induce more divergent reasoning paths, where achieving high consensus remains difficult. Nevertheless, even in these harder settings, RAST offers substantial improvements over the base model, demonstrating that reasoning diversity and consensus can be meaningfully enhanced without full RL training.

C.2 Response Length

To better understand the behavioral effects of RAST on model generation, we examine the average response length per problem across six mathematical reasoning benchmarks, as shown in Table 6. We report the number of output tokens generated by RAST under each setting.

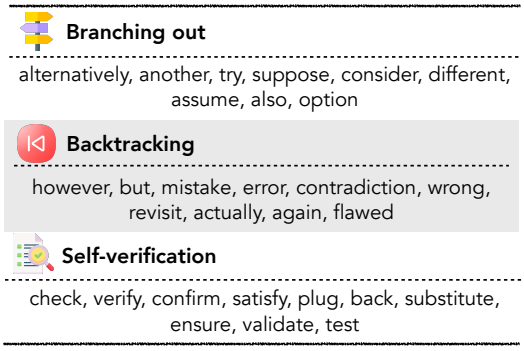

Figure 9: The set of manually curated reasoning tokens that corresponds to three key reasoning behaviours.

Firstly, we observe that the RL-trained model generally increases the output length compared to the base models, suggesting that it encourages more verbose or exploratory reasoning paths. This behavior aligns with the goal of RL to promote step-by-step reasoning and self-verification, which naturally results in longer outputs as the model articulates intermediate steps and justifications. We find that RAST inherits this trait: applying logit deltas from RL-trained experts to base models generally leads to increased response lengths, particularly when using deltas from much smaller expert models (e.g., $\Delta R_{1.5B}$). In some cases, the response length under RAST even exceeds that of the corresponding RL-trained model. For example, on AMC and GSM8K, Qwen-2.5-7B augmented with $\Delta R_{1.5B}$ produces significantly longer outputs than both its base and RLZero counterparts, reaching an average of 1362.8 and 354.9 tokens, respectively.

Additionally, we found that the performance of each setting is generally negatively correlated with the length of the generated outputs. Specifically, the length of generated outputs is always the shortest with RAST when we apply ΔR_{14B} than $\Delta R_{1.5B}$ with 32B base models. More interestingly, we found that the best performance achieved using RAST usually comes with the shortest length, indicating that RAST can achieve both efficiency and effectiveness if configured properly. This also brings up another door for the recent topic that try to compress the reasoning trajectories of RL-tuned models [65, 73, 3, 64, 42].

Overall, these results demonstrate that RAST not only activates reasoning behaviors but also affects the generation style. This controllability opens promising directions for future work in tuning the verbosity and structure of generation by manipulating transfer signals, and supports the broader narrative that RAST serves not just as a reasoning enhancer but also as a tool for decoding-time style modulation.

C.3 Empirical Token Signals of Reasoning Activation

To further examine how RAST elicits reasoning behaviors during generation, we perform a token-level analysis focusing on linguistic traces that reflect three hallmark reasoning behaviors: (i) *branching out*, (ii) *backtracking*, and (iii) *self-verification* as previously mentioned in Section 1. For each behavior, we manually curated a set of representative tokens based on prior qualitative observations and related work [11, 50, 60]. These tokens serve as behavioral signatures that may surface when the model engages in complex reasoning. The complete set of curated tokens are displayed in Figure 9.

We compute the frequency of these tokens in all 32 model output trajectories across six mathematical reasoning benchmarks, comparing the base model $\mathcal{M}_{base}$, RL-trained ceiling model $\mathcal{M}_{RL}$, and RAST with ΔR_{14b} applying to 32B base models. Figure 10 presents the normalized occurrence rates of each token category across different models. Two key trends emerge:

Dataset-specific reasoning emphasis. Different benchmarks accentuate different types of reasoning behaviors. For instance, **AIME 2024** and **Olympiad Bench** exhibit a pronounced increase in *branching out* and *backtracking* tokens, indicating that these tasks may demand exploring alternative

Table 6: The response length of output generated per problem by RAST on six mathematical reasoning benchmarks.

Models	Math500	AIME24	AMC	Minerva	Olympiad	GSM8K
Qwen-2.5-32B	566.9	1446.5	782.9	757.8	1103.4	275.6
$+\Delta R_{1.5B}$	685.1	1417.5	1024.2	799.5	978.3	333.1
$+\Delta R_{7B}$	614.5	1033.2	895.8	635.4	870.1	307.8
$+\Delta R_{14B}$	591.9	1164.6	863.9	605.7	886.9	297.6
32B-RLZero	659.2	1183.5	940.4	655.8	992.4	307.2
Qwen-2.5-14B	803.8	1138.9	820.2	921.5	1237.0	227.5
$+\Delta R_{1.5B}$	706.6	2092.0	1131.9	1070.6	1438.1	337.6
$+\Delta R_{7B}$	606.9	1092.4	919.1	636.3	889.4	309.8
14B-RLZero	682.7	1477.8	1034.9	667.1	1068.4	318.7
Qwen-2.5-7B	651.3	1765.9	756.0	657.2	1033.2	263.9
$+\Delta R_{1.5B}$	862.7	2127.4	1362.8	944.6	1123.5	354.9
7B-RLZero	682.6	1410.5	1074.6	731.7	1033.7	330.3

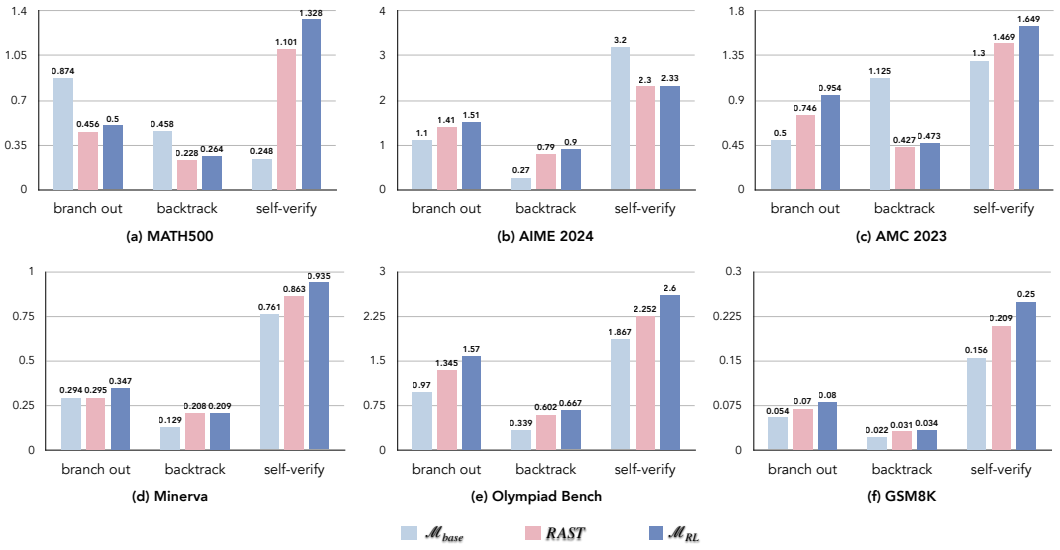

Figure 10: Normalized frequencies of reasoning-related tokens across three models ($\mathcal{M}_{base}$, RAST, and $\mathcal{M}_{RL}$) over six benchmarks. Each subfigure reflects a different reasoning behavior category.

solution paths and revisiting previous steps. In contrast, datasets like **AMC 2023** and **MATH500** emphasize *self-verification*, with higher frequencies of verification-related tokens such as "check" or "confirm". This variation suggests that reasoning demands are not uniform across benchmarks, and token-level analysis can surface behavior-specific task signals.

RAST steers base models closer to RL-trained behaviors. Across all datasets and reasoning categories, we observe that RAST consistently increases the frequency of reasoning-related tokens relative to $\mathcal{M}_{base}$ and more closely matches the RL-trained model $\mathcal{M}_{RL}$. This alignment is particularly clear in **Minerva**, **Olympiad Bench**, and **GSM8K**, where RAST nearly mirrors the behavior of $\mathcal{M}_{RL}$ in the *self-verification* dimension. These results support our central claim that the delta logit signal ΔR effectively induces reasoning traits without the need for full RL training on large-scale models.

Together, these findings offer empirical evidence that RAST not only activates latent reasoning capabilities within base models but also tailors such activation in a task-sensitive manner, approximating the behavioral signature of much costlier RL-trained experts.

D Memory Estimation Details

We estimate the memory considering tensor parallel and CPU offloading (since these are common tricks during training) based on the following dimensions: (i) model memory footprint (FP16), (ii) optimizer states, and (iii) activations & buffers.

Model Memory Footprint. To estimate the memory consumed by model parameters, we consider GRPO training with three model instances: policy, critic, and reference. For each, the parameter size is calculated as `(model size / tensor parallelism factor) × 2 bytes`, assuming FP16 precision. For example, a 14B model with tensor parallelism of 4 would require approximately `(14B / 4) × 2B × 3 = 21GB` per GPU. This accounts for only the static model weights without any optimizer states or intermediate activations.

Optimizer States with CPU Offloading. We assume DeepSpeed ZeRO Stage 3 is used to offload optimizer states entirely to CPU memory, which is a common practice in current RL training [75]. Under the Adam optimizer, each parameter typically requires two FP32 states, leading to a total memory footprint of approximately `2× model size × 4 bytes × number of models`. These optimizer states are excluded from GPU memory but are included in CPU memory estimates. For example, in a 14B GRPO setup, this results in approximately 156 GB of CPU RAM usage for the optimizer alone. In our paper, we mainly focus on the GPU memory overheads; therefore, if using CPU offloading, the memory requirement for optimizer states could almost be neglected.

Activations and Buffer Overhead. Activation memory is estimated based on common usage patterns for transformer-based LLMs under long context lengths (e.g., 2048 tokens) and moderate batch sizes. We assume gradient checkpointing is enabled to reduce activation memory, typically resulting in 12–25 GB usage per GPU depending on model size and training configuration. Additionally, we account for 5–8 GB per GPU for auxiliary memory needs such as gradients, residual connections, attention caches, and NCCL communication buffers. These components are summed to estimate total GPU memory usage across devices.

E Future Directions

In this section, we briefly discuss the potential future directions following RAST.

Ensemble Methods. One natural extension of RAST involves ensemble strategies [9] across multiple small-scale expert models. Given that each expert model may encode slightly different reasoning strategies depending on its training trajectory or initialization, aggregating their logit-level deltas could lead to more robust reasoning activation. This ensemble mechanism can be used to reduce variance, enhance generalization across tasks, and potentially adapt to unseen domains with improved resilience. We did a very initial exploration in this direction, by ensembling ΔR_{14B}, ΔR_{7B} and $\Delta R_{1.5B}$ to the 32B base model of Qwen2.5 on MAHT500. We found that the results is actually around 75.6, which does not outperform RAST with a single ΔR_{14B}. We suspect the primary reason is due to the similarity reasoning behaviour encoded in ΔR across scales in the same Qwen model family. Therefore, the simple ensembling approach will hurt the performance, and also bring much memory overheads for inference. However, we argue that this is still an interesting direction for exploration if we could identify unique and diverse reasoning behaviors of different models before ensembling.

LoRA from Small Models. Another intriguing direction is to bridge the output-space corrections from RAST back into the parameter space through low-rank adaptation (LoRA) [21]. Instead of applying logit deltas directly in the decoding phase, we could naturally distil a lightweight LoRA module [76] for each RL-tuned model to imitate the adjustments suggested by smaller RL-tuned models. We may even build reasoning-centric LoRA hub [22] that enables cross-reasoning-behavior generalization and flexible reasoning pattern combination for a more controllable reasoning setting.

Beyond Reasoning. While RAST focuses on reasoning activation, the core idea of activating the reasoning behaviors from smaller RL-tuned models via output-space alignment may generalize to other capabilities, such as code generation, instruction following, or factual grounding. Future work

may explore how RAST-style activation compares with or complements other alignment techniques, including preference-based fine-tuning or reward modeling.

F Limitations

While RAST demonstrates strong empirical performance and introduces a practical paradigm for decoding-time reasoning enhancement, it also comes with several limitations that suggest directions for future research.

Lack of Theoretical Understanding. Our method is largely motivated by empirical observations and intuition about how reasoning behaviors are reflected in output distributions. However, the theoretical foundations for why logit-level adjustments from small RL-tuned models can be activated effectively across model scales remain underexplored. A deeper understanding of when and why such activation works — and its potential failure modes — would help establish more rigorous guarantees and improve method design.

Limited Gains on More Difficult Benchmarks. Although RAST consistently improves performance across a range of reasoning datasets, the improvements on more challenging tasks, such as AIME, are relatively modest. These datasets often involve abstract reasoning, multi-step derivations, or domain-specific heuristics that may not be sufficiently captured by smaller expert models. This limits the degree of reasoning behavior activation and suggests that RAST may benefit from combining with more targeted adaptation techniques.

Computational Trade-offs and Expert Quality Dependency. Despite avoiding full RL fine-tuning on large models, RAST still requires access to a reasonably strong small expert model trained with RL, which can be computationally expensive to obtain. Furthermore, the quality and generalization ability of RAST are inherently tied to the effectiveness of this small expert. If the expert model is poorly aligned or fails to exhibit robust reasoning behaviors, the transferred deltas may provide little benefit.